ChemComm

Chemical Communications

www.rsc.org/chemcomm

Volume 49 | Number 95 | 11 December 2013 | Pages 11119–11234

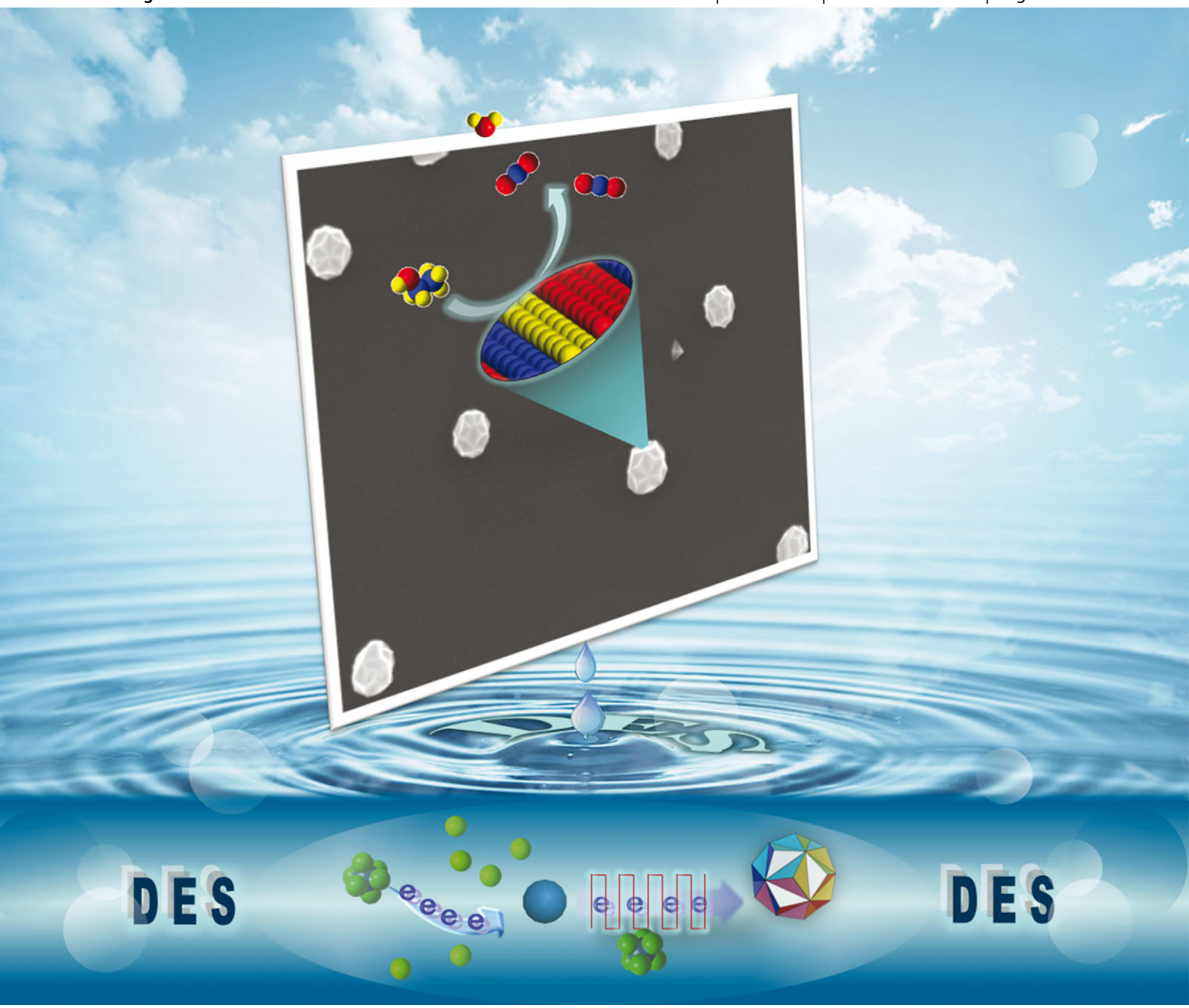

ISSN 1359-7345

RSC Publishing

COMMUNICATION

Shi-Gang Sun *et al.*

Electrochemically shape-controlled synthesis in deep eutectic solvents: triambic icosahedral platinum nanocrystals with high-index facets and their enhanced catalytic activity

ChemComm

RSC Publishing

COMMUNICATION

View Article Online
View Journal | View Issue

Cite this: *Chem. Commun.*, 2013, **49**, 11152

Received 24th August 2013,
Accepted 18th September 2013

DOI: 10.1039/c3cc46473c

www.rsc.org/chemcomm

Electrochemically shape-controlled synthesis in deep eutectic solvents: triambic icosahedral platinum nanocrystals with high-index facets and their enhanced catalytic activity†

Lu Wei,[a] Zhi-You Zhou,[a] Sheng-Pei Chen,[a] Chang-Deng Xu,[a] Dangsheng Su,[bc] Manfred Erwin Schuster[c] and Shi-Gang Sun*[a]

Pt triambic icosahedral nanocrystals (TIH NCs) enclosed by {771} high-index facets were successfully synthesized electrochemically, for the first time, in ChCl–urea based deep eutectic solvents, and exhibited higher electrocatalytic activity and stability towards ethanol electrooxidation than a commercial Pt black catalyst.

Shape-controlled synthesis of platinum (or other noble-metallic) nanocrystals (NCs) enclosed by high-index facets has attracted, in recent years, intense interest due to their fascinating properties and potential applications such as in catalysis, surface-enhanced Raman scattering (SERS), the (petro)chemical industry and fuel-cell technology.[1] As is well known, high-index facets possess high densities of atomic steps, ledges, and kinks, which can all contribute as highly active sites to breaking of chemical bonds such as C–C bonds. Therefore, the metal NCs with high-index facets generally exhibit higher catalytic activities than those with only low-index facets, such as {111} or {100} facets.[1d] For example, we have determined that the tetrahexahedral (THH) Pt NCs enclosed by {*hk*0} high-index facets exhibit excellent electrocatalytic activity for formic acid and ethanol oxidation.[2] Moreover, several groups have reported that the concave Pt NCs with high-index facets also have superior catalytic activities.[3] Although such high-index facets are fascinating and significant for the enhancement of reactivity, they are usually eliminated during their growth in a conventional synthesis process, due to the thermodynamics that drives the NCs minimizing their surface energy. For this reason, the shape-controlled synthesis of NCs bound with high-index facets is still a great challenge.

Recently, we have found that deep eutectic solvents (DESs) are alternative media in shape-controlled synthesis of high-index faceted metal NCs. For instance, the star-shaped Au NCs bound with {311} and vicinal high-index facets were successfully synthesized by a chemical reduction route.[4] Furthermore, novel concave THH Pt NCs enclosed by {910} high-index facets with enhanced catalytic activity have been prepared by an electrochemical method.[5] DESs are a new class of eutectic-based ionic liquids (ILs), which can be produced using quaternary ammonium or phosphonium salts complexed with different hydrogen bond donors such as amides, carboxylic acids and polyols.[6] Compared to conventional ILs, the DESs are non-toxic, biodegradable, environmentally friendly and have additional advantages such as easy preparation in high purity, stability in water and air, and low cost. Because of their remarkable physicochemical properties, the DESs have received extensive attention due to their broad applications in catalysis, electrochemistry and electrodeposition, as (co-)solvents in organic and inorganic syntheses, as well as in biocatalysis.[7]

In the current communication, we report the synthesis of triambic icosahedral (TIH) Pt nanocrystals (TIH Pt NCs), for the first time, in choline chloride (ChCl)–urea based DES by applying the electrochemical method. It has been determined that the TIH Pt NCs are bound by {771} high-index facets and exhibit higher electrocatalytic activity than commercial Pt black for ethanol oxidation. In a typical preparation, the TIH Pt NCs were directly electrodeposited on a glassy carbon (GC) electrode in 19.3 mM H_2PtCl_6–DES solution at 80 °C as illustrated in Scheme 1 (synthetic details are given in the ESI†). It has been

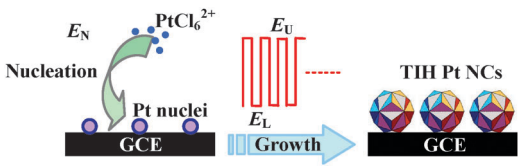

Scheme 1 Illustration of the programmed electrodeposition method for preparation of TIH Pt NCs.

[a] *Energy Research School, State Key Laboratory for Physical Chemistry of Solid Surfaces, Department of Chemistry, College of Chemistry and Chemical Engineering, Xiamen University, Xiamen 361005, China. E-mail: sgsun@xmu.edu; Fax: +86 592-2180181*
[b] *Shenyang National Laboratory for Materials Science, Institute of Metal Research, Chinese Academy of Sciences, 72 Wenhua Road, Shenyang 110016, China*
[c] *Fritz-Haber Institute of the Max-Planck-Society, Department of Inorganic Chemistry, Faradayweg 4-6, Berlin 14195, Germany*

† Electronic supplementary information (ESI) available. See DOI: 10.1039/c3cc46473c

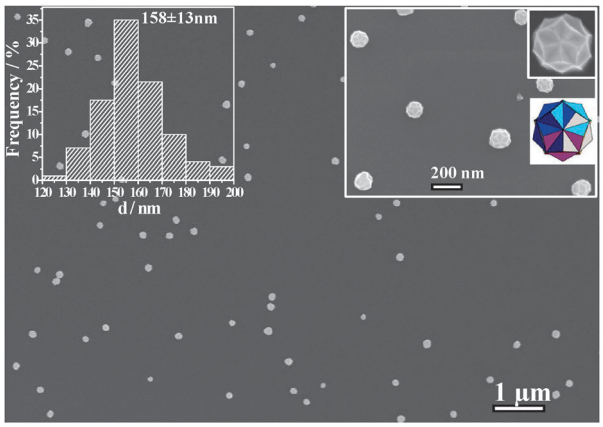

Fig. 1 Low-magnification SEM image of TIH Pt NCs electrodeposited on GC in 19.3 mM H_2PtCl_6–DES solution at 80 °C by a programmed electrodeposition routine: $E_N = -1.8$ V for 45 s, $E_L = -1.3$ V and $E_U = 0.3$ V at $f = 10$ Hz for growth for 15 min. The insets show the particle size histogram, high-magnification SEM image of TIH Pt NCs and the model of TIH shape, respectively.

shown that the square wave potential was an effective and facile way to tune nanocrystal surface structure by adjusting E_U and E_L.[2,5,8]

The as-prepared TIH Pt NCs were extensively examined by scanning electron microscopy (SEM, S-4800, Xiamen University) and transmission electron microscopy (TEM, FEI Titan 80-300 equipped with an image-Cs corrector, Fritz-Haber Institute of the Max-Planck-Society), as displayed in Fig. 1 and Fig. S1 in ESI.† It can be clearly seen that star shaped monodispersed polyhedral Pt NCs have been produced in high uniformity, and their size is measured to be 158 ± 13 nm. There are many symmetrical and nonerratic pyramids present on the surface of crystals. The high-magnification SEM image of Pt NCs and the corresponding TIH model along the direction of five-fold symmetry sufficiently illustrated that the as-synthesized Pt NC has a triambic icosahedral (TIH) shape. As illustrated in Fig. S2 (ESI†), the TIH polyhedron consists of a growing triangular pyramid on each of the twenty exposed (111) facets of an icosahedron.

To further characterize the surface structure of the TIH Pt NCs, TEM as well as HRTEM were carefully carried out by tuning the viewing angle, in order to determine the surface atomic arrangement of the edge-on facets. Fig. 2a demonstrates that the optimal projection direction of the TEM image for viewing the TIH Pt NC is along the [011] direction, as evidenced by the corresponding selected area electron diffraction (SAED) pattern (Fig. 2b) and the geometric model in Fig. 2c, which

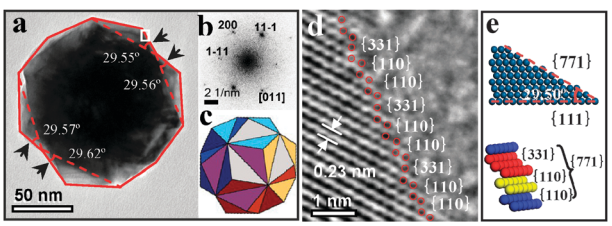

Fig. 2 (a) TEM image taken along the [011] direction, (b) SAED pattern, and (c) model of TIH Pt NCs along the [011] direction. (d) High-resolution TEM image of the area in the white box in Fig. 2a. (e) Atomic models of the Pt{771} plane.

results in a two-fold symmetry. To identify the Miller indices of the facets on TIH Pt NCs, one approach is to measure the projection angles between the four edge-on facets, which are indicated by the black arrows (Fig. 2a), and the corresponding {111} planes of icosahedrons underneath that are represented by the dashed lines in Fig. 2a (see details in Fig. S2 of ESI†). The angles between the four edge-on facets and the corresponding {111} planes are measured to be 29.55°, 29.56°, 29.62° and 29.57° as indicated in Fig. 2a. The theoretical values of angles between different high-index planes with Miller indices {*hkl*} and the {111} planes are listed in Table S1 (ESI†). In comparison to the measured angles with the values listed in Table S1 (ESI†), the facets enclosing the as-prepared TIH Pt NCs should be high-index {771} planes. Fig. 2d displays an HRTEM image recorded from the boxed area in Fig. 2a. It can be clearly observed that the surface atomic arrangement of Pt NCs possesses the feature of a high-index {771} plane, *i.e.* its configuration consists of periodically one {331} subfacet and two {110} subfacets. The HRTEM observation is consistent with the atomic model of a single crystal (771) (Fig. 2e). It is obvious that such high-index facets contain a high density of step atoms. As seen from Fig. 2d, furthermore, a lattice spacing of 0.23 nm agrees with the distance between two {111} planes of Pt, implying that the growth direction of the triangle pyramids present on the surface of NCs is along the [111] crystallographic direction.

To understand clearly how the TIH Pt NCs were developed during their growth by electrodeposition, the intermediate Pt NCs grown at different growth times were characterized by using SEM and TEM (Fig. S3, ESI†). The defective TIH shaped Pt NCs were obtained in 5 min (Fig. S3a and S3e, ESI†). Remarkably, upon increasing the growth time to 10 min or longer, the defective TIH shape grew into a perfect TIH morphology (Fig. S3b–d and f–h, ESI†). The corresponding sizes for the growth times of 5, 10, 15, and 30 min are measured, respectively, to be 70 ± 3, 106 ± 16, 158 ± 13, and 225 ± 28 nm (Fig. 1 and Fig. S4, ESI†). It is found that the feature of TIH shape is maintained regardless of the particle size when the growth time exceeds 10 min, although the facets are better defined or more easily assignable for larger particles.

For the successful formation of the TIH Pt NCs, the control of E_U and E_L and the nucleation are the key synthetic levers. When the nucleation step was skipped, the products consist of mixed morphologies including cubes and triangular bipyramids (Fig. S5 and S6, ESI†), meaning that the TIH Pt NCs hardly grew on the GC electrode without the nucleation process. To investigate the influence of E_U on the formation of TIH Pt NCs, various values of E_U were applied for the synthesis of Pt NCs under otherwise identical experimental conditions (Fig. S7, ESI†). It was found that the concave cubic Pt NCs of about 100 nm in size were produced at an E_U of 0 V (*vs.* Pt reference electrode). When E_U is 0.05 V, however, the product consists of mixed morphologies including concave cubes and irregular particles with larger size. Interestingly, upon further increasing the E_U to 0.10 V, defective TIH Pt NCs about 150 nm in size were formed except concave cubes NCs with smaller size (about 70 nm). In the cases of an E_U of 0.20 and 0.40 V, the morphologies of the products have no difference with respect to that shown in Fig. 1 for 0.30 V, except the sizes. However, a fewer imperfect TIH Pt NCs with larger size were obtained by further

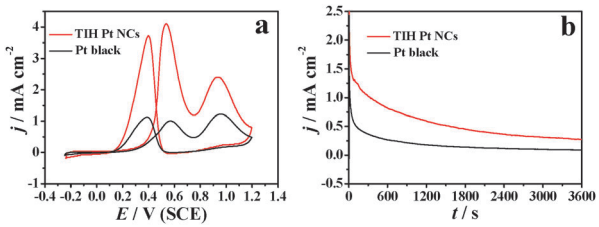

Fig. 3 (a) Cyclic voltammograms (50 mV s^{-1}) and (b) chronoamperometric curves, measured at 0.45 V (*vs.* SCE), of ethanol oxidation on TIH Pt NCs (red line) and the commercial Pt black catalyst (black line) in 0.1 M ethanol + 0.1 M $HClO_4$ solution.

augmenting E_U to 0.50 V. This observation suggests that the morphology of the product is highly dependent on E_U. Although the role of E_U is, as of now, unclear, the formation of TIH NCs might originate from the selective binding of urea species from DES at the higher E_U on these {*hhl*} high-index facets of Pt NCs during growth. Climent and co-workers have demonstrated potential-dependent changes in the bonding of urea at the Pt(110), Pt(111) and Pt(*hhl*) stepped surfaces that contain (111) terraces and (110) steps, with N-bonded and O-bonding urea predominating at low and high coverages, respectively.[9] Fig. S8 (ESI†) shows the SEM images of Pt NCs generated at different E_L, under otherwise identical experimental conditions. At an E_L of −1.40 V (*vs.* Pt reference electrode), truncated TIH Pt NCs were formed. When the E_L is −1.20 V, the product consists of mixed morphologies including imperfect TIH and polyhedrons such as a cube and a triangular bipyramid. Upon further increasing the E_L to −1.10 V, cubic Pt NCs with clusters on their surface were observed. It is worthwhile noting that the perfect TIH Pt NCs were formed exclusively at an E_L of −1.30 V (Fig. 1). However, when applying a constant potential at E_L, a few Pt nanoflowers with sharp petals were obtained (Fig. S8d, ESI†). These results indicate that the formation of TIH Pt NCs with high-index {*hhl*} facets is controlled by the dynamic interplay between the growth at E_L and surface adsorption of urea species at E_U, as well as the indispensable nucleation process.

To evaluate the electrocatalytic properties of as-prepared TIH Pt NCs with high-index facets, the electrocatalytic oxidation of ethanol was chosen as probe reaction, because stepped surfaces have a high reactivity for breaking the C–C bond and oxidation of adsorbed CO fragments involved in ethanol oxidation.[10] Fig. 3 compares cyclic voltammetry (CV) curves for electrooxidation of ethanol on the TIH Pt NCs and the commercial Pt black catalyst. The oxidation current has been normalized to the electroactive surface area, which was measured from the electric charge of hydrogen adsorption–desorption on Pt surfaces (Fig. S9, ESI†). As shown in Fig. 3a, the ethanol electrooxidation on TIH Pt NCs yields two current peaks near 0.54 and 0.94 V (*vs.* SCE) in the positive-going potential scan, their peak current densities are 4.11 and 2.41 mA cm^{-2}, respectively. The corresponding values obtained on the Pt black catalyst are only 1.01 and 1.24 mA cm^{-2}. It is evident that the electrocatalytic activity of the TIH Pt NCs for ethanol oxidation is 2–4 fold higher than that of the Pt black catalyst. Fig. 3b exhibits the current–time curves of ethanol oxidation at 0.45 V (*vs.* SCE). The steady current densities (t = 3600 s) of ethanol oxidation on the TIH Pt NCs and the Pt black catalyst are measured to be 0.28 and 0.09 mA cm^{-2}, respectively. This result clearly demonstrates that the long-term electrocatalytic activity of the TIH Pt NCs for ethanol oxidation is still superior to that of the Pt black catalyst. The enhancement in electrocatalytic activity and stability of the TIH Pt NCs is attributed to the exposed {771} high-index facets enclosed by the TIH Pt NCs, which contain a high density of atomic steps.

In summary, TIH Pt NCs enclosed by {771} high-index facets were successfully synthesized electrochemically, for the first time, in ChCl–urea based DES. The optimized NC growth kinetics, by controlling the dynamic interplay between the growth at E_L and surface adsorption at E_U, plays a decisive role in the formation of the TIH Pt NCs. The as-prepared TIH Pt NCs exhibit higher electrocatalytic activity and stability than the commercial Pt black catalyst for ethanol oxidation owing to their high-density stepped atoms. This study is of significance for shape-controlled synthesis of other noble metal NCs with high-index facets in DESs, as well as in some potential applications of electrocatalysis, electrochemical sensors and fuel cells.

This study was supported by the Natural Science Foundation of China (21021002).

Notes and references

1 (*a*) Z. W. Quan, Y. X. Wang and J. Y. Fang, *Acc. Chem. Res.*, 2013, **46**, 191; (*b*) H. Zhang, M. S. Jin and Y. N. Xia, *Angew. Chem., Int. Ed.*, 2012, **51**, 7656; (*c*) L. Zhang, W. X. Niu and G. B. Xu, *Nano Today*, 2012, **7**, 586; (*d*) N. Tian, Z. Y. Zhou and S. G. Sun, *J. Phys. Chem. C*, 2008, **112**, 19801.
2 N. Tian, Z. Y. Zhou, S. G. Sun, Y. Ding and Z. L. Wang, *Science*, 2007, **316**, 732.
3 (*a*) Z. C. Zhang, J. F. Hui, Z. C. Liu, X. Zhang, J. Zhuang and X. Wang, *Langmuir*, 2012, **28**, 14845; (*b*) L. Zhang, D. Q. Chen, Z. Y. Jiang, J. W. Zhang, S. F. Xie, Q. Kuang, Z. X. Xie and L. S. Zheng, *Nano Res.*, 2012, **5**, 181; (*c*) X. Q. Huang, Z. P. Zhao, J. M. Fan, Y. M. Tan and N. F. Zheng, *J. Am. Chem. Soc.*, 2011, **133**, 4718; (*d*) T. Yu, D. Y. Kim, H. Zhang and Y. N. Xia, *Angew. Chem., Int. Ed.*, 2011, **50**, 1.
4 H. G. Liao, Y. X. Jiang, Z. Y. Zhou, S. P. Chen and S. G. Sun, *Angew. Chem., Int. Ed.*, 2008, **47**, 9100.
5 L. Wei, Y. J. Fan, N. Tian, Z. Y. Zhou, X. Q. Zhao, B. W. Mao and S. G. Sun, *J. Phys. Chem. C*, 2012, **116**, 2040.
6 (*a*) A. P. Abbott, G. Capper, D. L. Davies, R. K. Rasheed and V. Tambyrajah, *Chem. Commun.*, 2003, 70; (*b*) A. P. Abbott, D. Boothby, G. Capper, D. L. Davies and R. K. Rasheed, *J. Am. Chem. Soc.*, 2004, **126**, 9142; (*c*) A. P. Abbott, R. C. Harris and K. S. Ryder, *J. Phys. Chem. B*, 2007, **111**, 4910; (*d*) M. A. Kareem, F. S. Mjalli, M. A. Hashim and I. M. AlNashef, *J. Chem. Eng. Data*, 2010, **55**, 4632.
7 Q. H. Zhang, K. D. O. Vigier, S. Royer and F. Jérôme, *Chem. Soc. Rev.*, 2012, **41**, 7108.
8 (*a*) N. Tian, Z. Y. Zhou, N. F. Yu, L. Y. Wang and S. G. Sun, *J. Am. Chem. Soc.*, 2010, **132**, 7580; (*b*) Y. Y. Li, Y. X. Jiang, M. H. Chen, H. G. Liao, R. Huang, Z. Y. Zhou, N. Tian, S. P. Chen and S. G. Sun, *Chem. Commun.*, 2012, **48**, 9531.
9 V. Climent, A. Rodes, R. Albalat, J. Claret, J. M. Feliu and A. Aldaz, *Langmuir*, 2001, **17**, 8260.
10 (*a*) J. Souza-Garcia, E. Herrero and J. M. Feliu, *ChemPhysChem*, 2010, **11**, 1391; (*b*) F. Colmati, G. Tremiliosi-Filho, E. R. Gonzalez, A. Berná, E. Herrero and J. M. Feliu, *Phys. Chem. Chem. Phys.*, 2009, **11**, 9114.

